Carbohydrate Polymers 369 (2025) 124310

Contents lists available at ScienceDirect

Carbohydrate Polymers

journal homepage: www.elsevier.com/locate/carbpol

Eco-design of cellulose nanocrystals through ESCAPE method at lab-scale

Gloria Nicastro [a], Ario Fahimi [b], Alain Dufresne [c], Ehsan Vahidi [b], Carlo Punta [a,*], Elza Bontempi [d,*]

[a] Department of Chemistry, Materials and Chemical Engineering, "Giulio Natta", Politecnico di Milano, via Luigi Mancinelli 7, Milano, Italy
[b] Department of Mining and Metallurgical Engineering, Mackay School of Earth Sciences and Engineering, University of Nevada, Reno, NV, USA
[c] University of Grenoble Alpes, CNRS, Grenoble INP, LGP2, F-38000 Grenoble, France
[d] INSTM and Department of Mechanical and Industrial Engineering, University of Brescia, Via Branze 38, 25123 Brescia, Italy

ARTICLE INFO

Keywords:
Nanocellulose
Cellulose nanocrystals
Eco-design
Sustainable production
Deep eutectic solvent
Tap water

ABSTRACT

Cellulose nanocrystals (CNC) are produced mainly following top-down procedures by cleaving the hierarchical structure of cellulose. Herein, we investigate and compare, at lab scale, two different processes for CNC production: the standard one, based on acidic treatment by H_2SO_4, and an alternative approach involving an oxalic acid/choline chloride deep eutectic solvent (DES), with the aim of both verifying the allegedly "greener" impact of the latter protocol and of identifying those critical steps to intervene on for an appropriate process eco-design. CNC from both methods were produced and characterized in terms of chemical composition, surface charge, and morphology. At the same time, the sustainability of the lab-scale processes was evaluated using the "ESCAPE" tool. Considering the different energy mixes provided by two European countries (Italy and France), sustainability was assessed in terms of embodied energy (EE) and carbon footprint (CF). The DES-based process was found to be more sustainable due to its shorter purification time and higher mass recovery. These findings allowed to identify the most impactful steps in the synthesis processes, namely purification phases and water consumption. Targeted improvements of these steps reduced the overall environmental impact with minimal effect on the final chemical and physical properties of the materials.

1. Introduction

Cellulose is a high-molecular-weight semicrystalline biopolymer that includes both amorphous and crystalline domains, composed of β-D-glucopyranose units linked by β-1,4-glycosidic bonds (Habibi et al., 2010; Rana et al., 2021). It can be extracted from different sources, such as wood or discharged biomass (Pennells, Godwin, Amiralian, & Martin, 2020). The hierarchical cleaving of cellulose, following a "top-down" approach by deconstructing the elementary fibrils down to the nanoscale, leads to the formation of nanocellulose, mainly in the form of cellulose nanofibers (CNF), containing both crystalline and amorphous regions, and cellulose nanocrystals (CNC), where the amorphous region is removed. Both CNF and CNC are recognized for their outstanding properties, such as biodegradability, biocompatibility, and renewability (Rana et al., 2021), while ongoing studies confirm their overall (eco) safety (Esposito et al., 2024; Ong et al., 2017; Rusconi et al., 2024; Wang, Song, et al., 2020). Moreover, they exhibit remarkable physicochemical properties, including stiffness, optical transparency, and high reactivity, attributed to their high surface area (Trache et al., 2017). Due to these properties, CNC find applications in different fields, including drug delivery (Liu et al., 2023), art preservation (Xu et al., 2020), catalysis (Chen et al., 2024), cosmetics (Mendoza et al., 2021) and packaging, both as filler and strengthening additives (Dong et al., 2012) and as main components in coatings to impart barrier properties (Azeredo et al., 2017; Li et al., 2013).

The most diffused method for producing CNC consists in hydrolysis by means of different acids, including H_2SO_4, HCl, or H_3PO_4. The reaction mechanism for CNC isolation involves diffusion of H_3O^+ ions into

Abbreviations: EBP, Eucalyptus bleached pulp; H_2SO_4, Sulfuric acid; DES, Deep eutectic solvent; CnCl, Choline chloride; OxAc, Oxalic acid; LODP, Lower degree of polymerization; CNC, Cellulose nanocrystals; CNC-S, Cellulose nanocrystals produced by sulfuric acid; CNC-S-TAP, Cellulose nanocrystals produced by sulfuric acid with the use of tap water; CNC-DES, Cellulose nanocrystals produced by deep eutectic solvent; CNC-DES-TAP, Cellulose nanocrystals produced by deep eutectic solvent with the use of tap water; CUED, Cupriethylenediamine; ESCAPE, Evaluation of Sustainability of material substitution using CArbon footPrint by a simplifiEd approach; LCA, life cycle assessment; EE, Embodied energy; CF, Carbon footprint; GHG, Green-house gas.

* Corresponding authors.
E-mail addresses: carlo.punta@polimi.it (C. Punta), elza.bontempi@unibs.it (E. Bontempi).

https://doi.org/10.1016/j.carbpol.2025.124310
Received 10 July 2025; Received in revised form 14 August 2025; Accepted 28 August 2025
Available online 1 September 2025
0144-8617/© 2025 The Authors. Published by Elsevier Ltd. This is an open access article under the CC BY license (http://creativecommons.org/licenses/by/4.0/).

the amorphous region, promoting cleavage of β-1,4-glycosidic bonds. The hydrolyzation reaction has two different kinetics with respect to the amorphous and crystalline domains, with the amorphous region being hydrolyzed faster. Once the protons reach the cellulose chains, hydrolysis catalyzes the breaking of glycosidic bonds. Each acid affects CNC properties differently. The H_2SO_4 approach (Fig. 1A) promotes the formation of highly charged CNC capable of forming stable colloidal suspensions but characterized by reduced thermal stability. HCl leads to uncharged CNC, which consequently generate less stable colloidal suspensions but exhibit higher thermal stability. The H_3PO_3-mediated approach yields CNC with low charge density, offering a balance between colloidal and thermal stability. Other organic acids like maleic, oxalic, and formic ones have also been explored to avoid more hazardous acids without compromising CNC formation. These treatments produce functionalized CNC with good dispersibility and enhanced thermal stability. However, due to their pK_a values, they require longer reaction times and eventually additional pretreatments, thus increasing the overall energy consumption of the process (Tang et al., 2022).

An alternative approach to traditional acidic treatment consists in using deep eutectic solvents (DES) (Abbott et al., 2004; Amoroso et al., 2021). DES, typically formulated from cost-effective materials, offer numerous advantages, including easy synthesis, high biodegradability, negligible toxicity, and possible reuse. The most widely used DES for CNC extraction are formed by choline chloride (ChCl), in combination with a series of organic acids, such as oxalic acid (OxAc) (Fig. 1B). The reaction mechanism for extracting CNC with DES involves the dissociation of $[Ch]^+$ and $[Cl]^-$, which diffuse into the interstitial spaces between cellulose's amorphous and crystalline domains. $[Ch]^+$ interacts with oxygen atoms of the hydroxyl groups and oxygen atoms of the glucopyranose cycle, while $[Cl]^-$ targets the hydrogen atoms of the hydroxyl groups and the carbons of the glycosidic bonds, facilitating bond breakage. The presence of OxAc (or any other organic acid) leads to esterification of hydroxyl groups, facilitating the cleaving process.

It is important to highlight how the two processes just presented differ not only in the approach to obtain CNC, but also in the morphology, crystallinity and surface chemistry of the obtained products, as will be discussed later.

Other methods are reported in the literature for the isolation of CNC, such as ionic-liquid extraction, enzymatic hydrolysis, subcritical water processes, oxidative extraction, and mechanochemical treatments. However, up to date, these latter approaches are far from being produced on a larger or at least pilot scale due to their reliance on costly chemicals or high energy consumption.

While designing CNC synthetic processes, it is crucial to consider from the very beginning not only the advantages of using these products in a wide range of application fields, but also the possible implications associated with their production, mainly associated with the overall environmental impact of the process. Life Cycle Assessment (LCA) is an essential tool for evaluating the environmental impacts associated with all the stages of a product's life, starting from raw material extraction up to its final disposal or recycling (British Standards, 2020). Moreover, as highlighted by Corsi et al. (2023), LCA could represent a key tool for the eco-design of new (nano)materials, and it should be integrated from the earliest stages of product development to ensure safe solutions for the environment. In the last years, few studies referring to LCA analysis for CNC production have been reported (da Cruz et al., 2024). In particular, Zargar et al. (2022) evaluated two different approaches for CNC production, both consisting in an extraction with a bi- or tri-component DES composed of ChCl and OxAc and eventually *p*-toluenesulfonic acid. The results showed how the tri-component DES had a lower impact in terms of energy consumption, allowing for shorter reaction times and lower temperatures. However, these processes led to the production CNC with a low degree of purity, the final lignin content being higher than 50 %. Moreover, the comparison with the H_2SO_4-mediated approach was conducted on a completely different source, leading to the formation of lignin-free crystals. More recently, Hoo et al. (2024) reported an LCA analysis on several CNC production processes from cotton, considering H_2SO_4 as a benchmark to recognize the most sustainable procedure. A high number of parameters were considered, concluding that the DES-mediated extraction approach is a more sustainable alternative to the H_2SO_4-mediated one. Nevertheless, none of the reported analyses really took part to a proper eco-redesign in order to improve the environmental hotspots.

In fact, all the LCA outputs focus on selecting the more sustainable approach among the already reported ones, rather than suggesting optimization at the early stages and validating the proposed variations. This happens also because, despite its comprehensive approach, LCA often falls short in lab-scale evaluations due to limitations in data scope and scalability (Fahimi et al., 2022). Therefore, there is a pressing need to explore alternative methods to complement or enhance the traditional LCA approach, especially in the context of early-stage research and development phases.

The ESCAPE method, namely Evaluation of Sustainability of material substitution using CArbon footPrint by a simplifiEd approach (Ducoli et al., 2023), provides a tool for material scientists to assess and compare the sustainability of material synthesis at the lab scale. It was designed to evaluate the sustainability of new materials, focusing specifically on their synthesis processes and comparing them to natural resources or corresponding commercial chemicals. Its primary aim is to quantify sustainability by measuring embodied energy (EE) and CO_2 footprint (CF), two typical LCA indicators, thus providing a less resource-intensive tool when full LCA data are unavailable. A sustainability index is defined based on these parameters, with a positive index indicating higher sustainability of the new material. Data for these calculations are sourced from databases like CES Selector and Ecoinvent. The approach also incorporates country-specific equivalence factors for energy and emissions, accounting for local variations in energy mix. By evaluating all steps of the synthesis process, including chemical, mechanical, and thermal treatments, ESCAPE allows for customization and focuses on significant energy and emission contributions. This approach supports eco-design by identifying the most energy-intensive steps in the synthesis process at the lab scale, which means at a stage when proper redesign of the process is still possible. It can serve as a preliminary screening tool to evaluate material sustainability before conducting a full LCA (Bontempi, 2022). The advantages of the ESCAPE approach include its simplified and rapid assessment of sustainability, resource efficiency by avoiding the complexities of full LCA, and early decision support for researchers. It helps identify the most energy and emission-intensive steps in the synthesis process, guiding improvements and optimizations. Furthermore, by considering the energy mix of different countries, ESCAPE enables more accurate sustainability evaluations based on location. Overall, it acts as a valuable preliminary screening tool to determine the viability of new materials, facilitating early, informed decision-making in the development of eco-friendly technologies (Ducoli et al., 2023).

To date, the method has been primarily used to evaluate the sustainability of new recycling technologies (Bontempi, 2017; Ducoli et al., 2023; Fahimi et al., 2022). In this work, the ESCAPE approach is utilized for the first time to perform an eco-design analysis, specifically for CNC production. By comparing the two lab-scale methods, the approach identifies the more sustainable one and guides modifications to enhance sustainability in production. Literature reports qualitative analyses, like those of Tang et al. (2022) that compared the sustainability of five different CNC extraction techniques, in alignment with the twelfth principle of green chemistry. Their findings indicated that sulfuric acid and DES methods are the most advantageous in terms of reaction conditions, recyclability, waste generation, and general CNC properties. However, as stressed before, their analysis was qualitative. To build on this foundation, we here apply the ESCAPE model to conduct a quantitative sustainability analysis of CNC production at the lab scale.

We aim to delineate the sustainability of the two distinct CNC production approaches (H_2SO_4 versus DES) by examining and optimizing

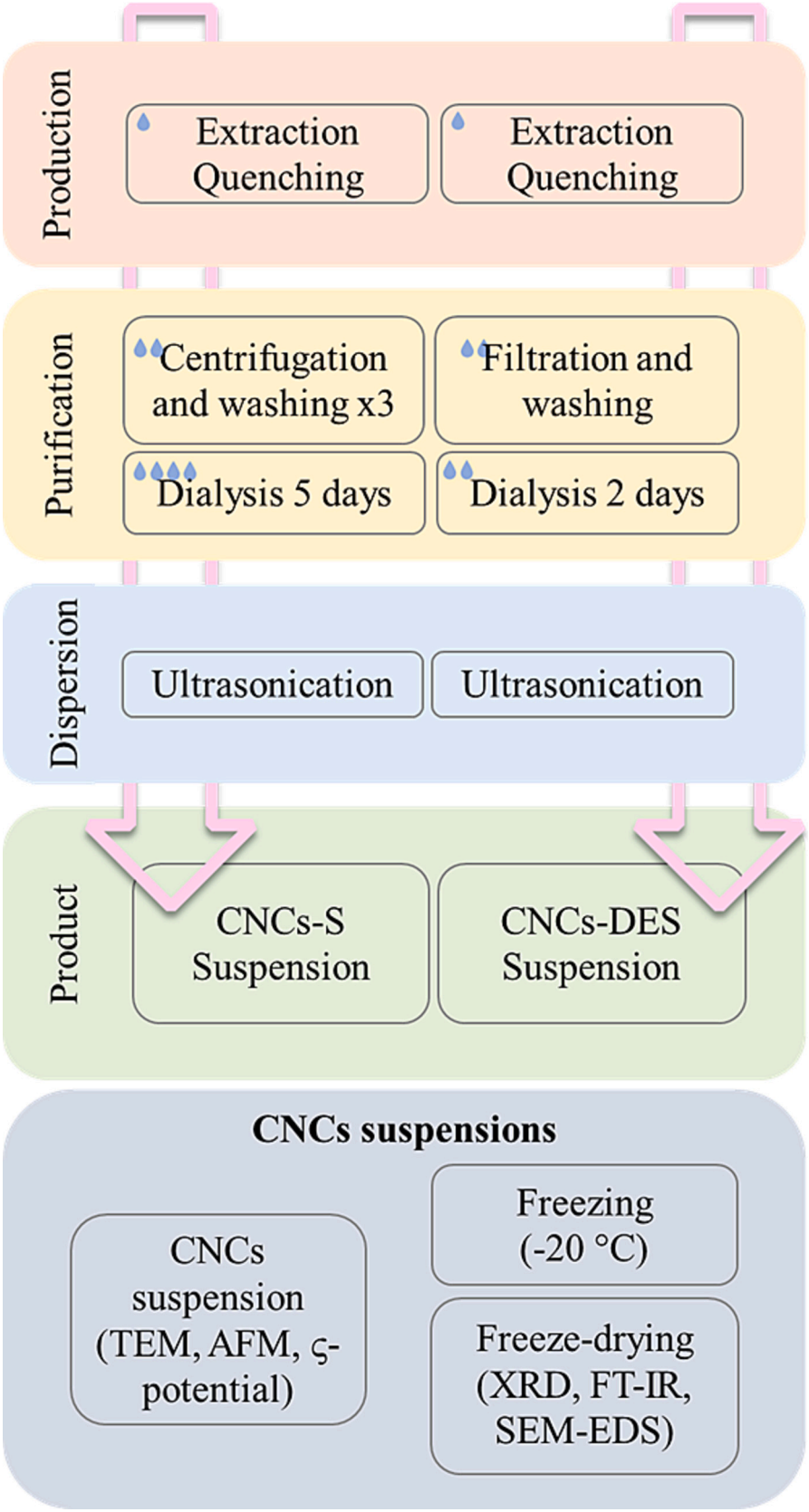

Fig. 1. CNC production processes: (a) H_2SO_4-based production, (b) DES-based production.

the most impactful steps involved in each process. Given that different production routes yield CNC with varying functional properties, we have also performed a comprehensive comparison of the chemical-physical properties of the final CNC products, and we have monitored if and how they change as a consequence of the eco-redesign process. This approach not only enhances our understanding of the environmental impact of each method but also provides insights into the potential for refining these processes for greater efficiency and sustainability.

2. Materials and methods

2.1. General

Eucalyptus bleached pulp (EBP) was provided by Mare S.p.A (Milan, Italy) and pre-treated by means of a Fourplex miller. H_2SO_4 (95.0–98.0 % aqueous solution) was purchased by Sigma-Aldrich, choline chloride (ChCl) and oxalic acid dihydrate (OA) by Fluorochem, dialysis membranes (12–14 kDa) by Roth and chloroform, NaOH and HCl by Carlo Erba.

2.2. Sulfuric acid hydrolysis and deep eutectic solvent extraction

CNC-S were prepared by H_2SO_4 hydrolysis, following a procedure previously described, with the introduction of some modifications (Aguayo et al., 2018) (Fig. 2a, Table S1). Briefly, 5 g of cellulose pulp was added to 200 mL of $H_2SO_{4(aq)}$ solution (50–64 % V//V) and stirred for 30–45 min, at 50 °C (350 rpm). Then, 10-fold reaction volume of water and ice mixture was used to quench the reaction. The obtained suspension was centrifuged three times at 10,000 rpm, for 20 min each. The suspension was dialyzed against distilled or tap water using a 12–14 kDa dialysis membrane until neutral pH was measured. Finally, to enhance CNC dispersion, the suspension was sonicated using an ultrasonicator Fisherbrand Model 505 Sonifier, with a 13 mm tip. To avoid bacterial growth, some drops of chloroform ($CHCl_3$) were added to 5 mL of the resulting suspension (Roohani et al., 2008) and stored at 4 °C, while the remaining suspension was frozen at −20 °C and lyophilized for further characterization. After ESCAPE optimization, the production process was kept similar, except for using tap water during the whole process and performing the dialysis without the magnetic stirring. In this case, the obtained material is named CNC-S-TAP.

For the DES treatment, 500 mg of pre-treated EBP was added to 50 g of DES, previously prepared in a one neck round bottomed flask (250 mL), by mixing under magnetic stirring a 1:1 molar ratio of ChCl (26.3 g) and OxAc (23.7 g) for 30 min at 95 °C (350 rpm). The extraction was conducted for 6 h at 95 °C. The suspension was quenched with a 5-fold volume of deionized or distilled water, filtered on 1 μm nylon filter under vacuum, further washed, re-dispersed in water, and ultrasonicated in an ice bath for 30 min (30 % amplitude). Finally, the suspension was dialyzed using a 12–14 kDa dialysis membrane for two days, frozen at −20 °C, and lyophilized, providing CNC-DES (Fig. 2b). CNC-DES-TAP was obtained by using tap water in the purification step and in the absence of magnetic stirring.

2.3. Characterization

The EBP sugar content was determined by H_2SO_4 hydrolysis. 350 mg of dry pulp was mixed with 3 mL of H_2SO_4 (72 % *V*/V) and kept under stirring for 1 h at 30 °C. 84 mL of distilled H_2O was then added, and the pulp was thermally treated in autoclave at 120 °C for 1 h, after which the suspension was filtered and analyzed.

The chemical composition of the starting material was evaluated using the Dionex ICS5000 ion exchange chromatographic system with a CarboPac PA10 column.

The degree of polymerization (DP_v) was obtained according to the ISO 5351-1:2010 (ISO, 2010). The pre-treated EPB was added to a glass vial together with 6 glass balls and water. The suspension was left overnight mechanically stirring in an orbital shaker. A solution of cupriethylenediamine (CUED) was then added to the suspension, which was further mechanically stirred for 2 h. The measure was performed in a glass viscometer, taking note of the efflux time, which is the time that the meniscus of the sample takes to go from the upper mark to the lower one. Each measure was repeated twice.

MorFi analysis was conducted by a Techpap MorFi Neo. 90 mg of EBP were soaked for 10 min in tap water and then blended for 10 min. The suspension was brought to 3 kg and divided into three beakers. The analyses were done on blended EBP and milled EBP in triplicate.

Dynamic Icon Atomic Force Microscopy (AFM) was used to measure the length and the width of CNC. Due to the cylindrical shape of CNC, the height and the diameter were assumed to be the same. The length and width were measured using ImageJ 1.54d software. The samples were prepared with a concentration of 1×10^{-3} to 1×10^{-4} % (m/V) by drop casting the ultrasonicated sample on a freshly cleaved mica plate, and letting it dry covered overnight. At least 100 measures were done for each sample.

Transmission Electron Microscopy (TEM) analysis was conducted by depositing droplets of dilute CNC suspensions onto glow-discharged carbon-coated TEM grids. After a few minutes, the excess liquid was blotted with filter paper and, prior to drying, the preparation was negatively stained with 2 % wt of uranyl acetate. The excess stain was

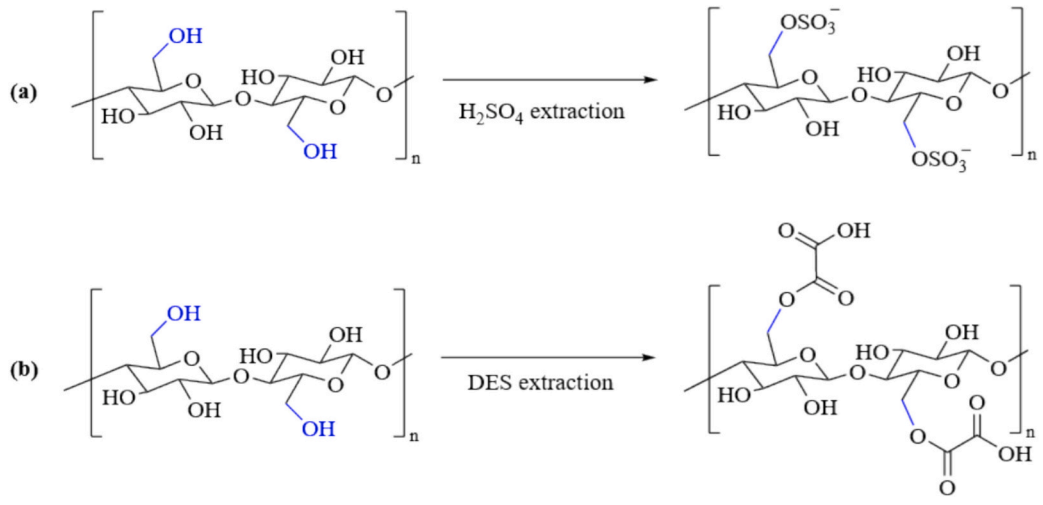

Fig. 2. Chemical structure of (a) CNC-S, and (b) CNC-DES.

blotted, and the specimen was allowed to dry. Images were recorded with a JEOL JEM-2100-Plus microscope operating at 200 kV equipped with a Gatan Rio 16 digital camera. The mean CNC value was assessed with ImageJ software, on a minimum of 100 measurements.

X-ray diffraction analysis was determined using an X'Pert Pro MDP instrument (Malvern Panalytical) in reflection mode with the Bragg Brentano geometry. The crystallinity index was determined using the Segal method (Segal et al., 1959), after background subtraction. The quantification was calculated as follows:

$$CI\% = \frac{I_{002} - I_{AM}}{I_{002}} \times 100 \quad (1)$$

where CI% is the crystalline index (%), I_{002} is the intensity of the crystalline peak at 22.5° and I_{AM} is the intensity of the amorphous peak, at 18°.

The freeze-dried samples were crushed by hand to obtain a powder material without increasing the amorphous portion. The amorphous sample was prepared by ball-milling using a Retsch CryoMill. 500 mg of the ground sample were put in the milling chamber, together with two milling balls. The treatment was performed at room temperature for 20 min.

The carboxylate and sulphate content of the CNC was obtained through conductometric titration, using a Hanna Instruments HI522-02 pH meter and conductometer. A known quantity of CNC was dispersed in 15 mL of a 0.01 M HCl solution (final concentration < 1 % m/V). As soon as the suspension was stabilized, the titration took place with 0.01 M $NaOH_{(aq)}$ solution. Data analysis is conducted by plotting the conductivity against the volume of $NaOH_{(aq)}$ solution and the relative carboxylate or sulphate content is obtained as follows:

$$C \text{ or } S = \frac{(V_2 - V_1) \times M_{NaOH}}{g_{CNC}} \quad (2)$$

where C represents the —COOH content; S, the —OSO_3H one; V_2 and V_1, the equivalent volumes of the added $NaOH_{(aq)}$ solution; M_{NaOH}, the precise NaOH molarity; g_{CNC}, the exact amount of CNC in suspension (Besbes et al., 2011).

Elemental analyses were conducted on EBP, CNC-S and CNC-DES, with a Costech ECS mod.4010.

Colloidal stability was tested with a Malvern Zetasizer Pro-Blue at 25 °C, according to Riva et al. (2024). All the solutions had a 1×10^{-3} % concentration. The CNC were dispersed in distilled water, at neutral pH. To enhance the homogeneity of the suspension, each sample was sonicated for 3 min at room temperature. The measurements were performed after a settling time of 1 min, and repeated five times, with 20 s settling time between each measure. The average ζ-potential was considered.

Thermogravimetric analysis (TGA) of all samples was obtained by a thermal analyzer Mettler Toledo (TGA/DSC 3+). The analyses were carried out in the atmosphere of air and nitrogen. The temperature increased from 25 °C to 900 °C, with a heating rate of 10 °C min^{-1}. Each sample weight was between 5 mg and 10 mg.

Attenuated Total Reflectance - Fourier Transform Infrared (ATR-FTIR) spectra were obtained on a Perkin-Elmer Spectrum 65 instrument (PerkinElmer, USA). Each sample was analyzed in air, in the dry form. The measures were performed in triplicates, from 4000 cm^{-1} to 600 cm^{-1}, with a scan rate of 32.

Scanning Electron Microscopy (SEM) analysis was conducted using a variable-pressure apparatus (SEM Cambridge Stereoscan 360) operating at 100/120 Pa, equipped with a Variable Pressure Scanning Electron VPSE detector. The electron beam operated at 20 kV with an intensity of 150 pA, and the focal distance was set at 8 mm. Specimens underwent analysis in High Vacuum mode post-metallization. Additionally, Energy Dispersive X-ray Spectroscopy (EDS) analysis was carried out utilizing a Bruker Quantax 200 6/30 instrument.

2.4. ESCAPE application

To evaluate the EE and CF of a material using the ESCAPE approach, several basic data points are required:

Material Data:

- Information on raw materials and reagents, including their source, quantity, and specific type.
- The quantity and type of water used in the process (e.g., distilled water, tap water).
- Embodied energy and CO_2 footprint values for each raw material and chemical, typically sourced from databases like CES Selector and Ecoinvent.

Process Data:

- Energy consumption: This includes the energy used in chemical, mechanical, and thermal treatments.
- The power ratings of all equipment used in the synthesis process, such as heaters, mixers, and dryers.

Operational Data:

- Duration of equipment use: the operating time for each piece of equipment used.
- Process efficiency: the energy conversion efficiency in the equipment used, particularly for electric-to-thermal and electric-to-mechanical energy conversions.

Country-Specific Data:

- The Energy Mix of the country where the synthesis process is performed, as it impacts the overall EE and CF calculations. This includes the percentages of electricity produced from fossil fuels, nuclear power, and renewable sources.

The condition parameters, along with the power ratings of laboratory equipment utilized, have been systematically detailed in Tables S2 and S3. This documentation ensures consistency in methodology across studies, facilitating accurate calculations and reliable comparisons between different experimental setups and research findings.

The data presented in Table S4 for the inventory of chemicals were acquired using the Simapro 9.5 Educational package, adopting the attributional approach and employing the point of substitution allocation method. These statistics were gathered from system processes within the comprehensive "transformation library of the latest Ecoinvent 3.9.1". Transformation processes encompass all the necessary inputs involved in creating a product or service, excluding transport processes, as well as inputs from associated emissions and resource extractions. The embodied energy data were derived using the single score method, which relies on cumulative energy demand sourced from non-renewable fossils. Meanwhile, the carbon footprint was assessed using the single score method according to IPCC standards, based on the Global Warming Potential (GWP) over 100 years. This measurement characterizes greenhouse gas emissions from non-renewable fossils and is expressed in kg CO_{2eq}. RoW stands for Rest of World, indicating the global average electricity mix.

We incorporated water's contribution by quantifying its EE and CF per kilogram, drawing from prior research conducted by Fahimi et al. in 2022 and Ducoli et al., 2023. Specifically, we considered various types of water, including distilled, deionized, and tap water, to comprehensively assess their environmental impact within the context of different scenarios for the production CNC under investigation.

Finally, Table S5 reports the energy mix, i.e. the combination of the various primary energy sources that are used to guarantee the energy needs of a specific geographic area. It includes fossil fuels (natural gas,

oil, and coal), nuclear energy, and renewable energy sources (such as wood, biomass, solar, wind, hydro, and geothermal). The data were derived from the reports of the non-profit organization Ember (Graham et al., 2025).

These primary energy sources are used for the counting of EE and CF derived from an electrical power rating of 1 kW, for 1 h of usage, evaluated for single world countries.

3. Results and discussion

3.1. Synthetic processes and chemical characterization

EBP composition resulted in 78 % cellulose, 21 % hemicellulose and 1 % Klason lignin. Each chemical treatment of the pulp was preceded by mechanical treatment with a Fourplex miller, aimed at reducing the size of the material and consequently obtaining a higher surface area in contact with either H_2SO_4 or DES. The average fiber length obtained by MorFi analyses was 680 ± 8,54 μm.

H_2SO_4 hydrolysis was performed according to (Aguayo et al., 2018) and optimized in terms of acid concentration, cellulose mass/aqueous solution volume ratio, and reaction time (Table S1). Reproducibility of CNC extraction was evaluated by conducting each process in triplicate. The reaction conditions which guaranteed the highest yields resulted in using a 50 % (*V*/V) aqueous solution of H_2SO_4 at 50 °C for 30 min, with a cellulose mass to volume ratio (m/V) of 1:40 (g/mL) (Table S1, entry 2), as any tentative to operate at lower cellulose to volume ratios led to fast depolymerization of the fiber with no cellulose mass recovery at the end of the process (Table S1, entry 1). We are aware that higher mass to volume ratios up to 1:10 are reported in literature (Chen et al., 2015), but it should be here highlighted that the process performance and processability highly depends on the characteristics of the starting source. That is why a complete characterization of cellulose source is here reported, while in most cases it is missing, limiting a correct comparison of the processes. However, a simulation by considering the higher 1:10 m/V is reported as attached file in the Supporting material, demonstrating that this aspect has a neglectable effect on the overall EE and CF. A mass recovery of 22 % was obtained, in line with what reported in literature (Gil-Castell et al., 2022). An increase either in reaction time or in acid concentration did not allow to obtain higher yields (Table S1, entries 3–7). On the contrary, harsher conditions led to a complete degradation of the starting material, obtaining a brownish pulp and lower to neglectable yields. The 22 ± 2 % yield value has been considered for ESCAPE sustainability evaluation. However, as depending on the starting source the final yields reported in literature range from 20 % to 75 % (Vanderfleet & Cranston, 2021), scenarios where yields were considered equal 100 % have been also simulated.

The DES-based method was referred to the ones reported in the literature (Douard et al., 2022; Liu et al., 2019; Wang, Li, et al., 2020) The preparation was conducted in a 1:100 (*w*/w) ratio of EBP to DES, which is the optimal ratio to allow reasonable stirring during the reaction, thus favoring a good EBP-DES contact. In fact, it is important to highlight the higher viscosity of DES with respect to water mediums, such as H_2SO_4 solutions. As traces of solvent remained in the product after CNC-DES filtration, dialysis was introduced to optimize the purification step. This second approach led to the formation of light brown CNC and showed higher mass recovery with respect to the acidic hydrolysis, reaching an average mass yield on 3 triplicates of 65 ± 7 % (considered for the ESCAPE sustainability evaluation). This value is totally consistent with what reported in the literature (Vanderfleet & Cranston, 2021). Nevertheless, also in this case scenarios where yields were considered equal to 100 % have been simulated as well.

Drying of CNC by lyophilization, whatever the selected approach for their production, also significantly impacts the overall production process due to massive energy consumption. However, up to now, it is the unique drying condition that allows a good re-dispersibility in water (Di Giorgio et al., 2020), as it has been reported that by exploiting simple vacuum drying a severe agglomeration of CNC occurs.

While with both procedures we obtained CNC, the chemical and physical properties of the two products differ. Elemental analyses revealed the presence of sulfur in CNC-S, suggesting partial sulfation by means of H_2SO_4. In fact, no sulfur was detected in either original EBP or CNC-DES (Table 1).

Conductometric titrations on CNC samples allowed to assess a possible —OSO_3H contribution for CNC-S (0.397 ± 0.019 $mmol_{-OSO3H}/g_{CNC}$) and a probable —COOH content for CNC-DES (0.482 ± 0.029 $mmol_{-COOH}/g_{CNC}$).

Fig. S1 and Fig. 3a show the thermal stability of EBP, CNC-S, and CNC-DES, as determined by TGA. The EBP thermal degradation occurs in two steps when the analysis is carried out in air. The first mass loss, below 250 °C, corresponds to the evaporation of the physically adsorbed water. The second mass loss coincides with the production of combustion gases due to dehydration and decarboxylation reactions. As for the mass loss in the range of 400 °C–500 °C, it can be attributed to the oxidative degradation of the char formed in the previous step (Ceylan et al., 2013). The trend of the analysis carried out under N_2 atmosphere is different. While the first weight loss corresponds to the evaporation of physically adsorbed water, the second and last weight loss is due to dehydration and decarboxylation reactions. The residue remaining after the analysis is higher than that observed under air atmosphere and this can be explained by the absence of the oxidative degradation step (Ceylan et al., 2013). The same experimental conditions were used for the analysis of CNCs. Fig. 3a reports the curves for CNC-S, under N_2 atmosphere and air. The trend in N_2 shows a first mass loss due to water loss, a second mass loss (239 °C) due to the degradation of the more labile CNC-charged surface, and a final mass loss (361 °C) due to the degradation of the more stable inner core of the CNC-S (Beck-Candanedo et al., 2005; Roman & Winter, 2004). Under an air atmosphere, the residual char derived from CNC degradation undergoes further oxidative degradation, leaving no mass in the crucible (241 °C, 315 °C, and 464 °C). As for CNC-DES, the trends are different. Under N_2 atmosphere, there is a first mass loss due to water evaporation, followed by an important second mass loss (332 °C) due to the degradation of CNC. In this case, a further mass loss as noticed for CNC-S is not observed. This is probably due to the fact that the surface of CNC-DES is not sulfated, and thus equally stable on the surface and in the inner core, and more thermally stable with respect to the previous samples. In the absence of oxygen, the residual char (ca. 20 % of the initial weight) is not further degraded by oxidative reactions. On the other hand, when operating under air atmosphere, additionally to the first CNC-DES degradation (318 °C), a further oxidative degradation occurs (471 °C), where the char is degraded to gases, leaving almost no mass in the crucible.

Fig. 3b shows the FT-IR spectra of EBP, CNC-S and CNC-DES. The broad band in the range 3600–3000 cm^{-1} corresponds to the —OH stretching of cellulose (Ciolacu et al., 2011). The peaks around 2900 cm^{-1} are due to the —CH_2 asymmetric and symmetric vibrations (Gil-Castell et al., 2022), while those at 1740 cm^{-1} are assigned to the stretching vibration of —C═O of carboxyl and acetyl moieties in hemicellulose (Carrillo et al., 2018). The peak at 1372 cm^{-1} is assigned to the —CH bending in cellulose I and hemicellulose (Aguayo et al., 2018; Carrillo et al., 2018). Lastly, around 890 cm^{-1} the absorption band is assigned to the C—O—C stretching of the glycosidic linkages between the glucose units (Carrillo et al., 2018; Ciolacu et al., 2011; Gil-Castell et al., 2022). In addition to the previously presented spectrum,

Table 1
Elemental analyses for EBP, CNC-S and CNC-DES.

Element	EBP	CNC-S	CNC-DES
N	<0.1	1.41 ± 0.010	0.50 ± 0.020
C	42.4 ± 0.010	40.4 ± 0.020	42.1 ± 0.30
H	9.14 ± 0.11	9.63 ± 0.15	9.04 ± 0.10
S	–	1.22 ± 0.070	–

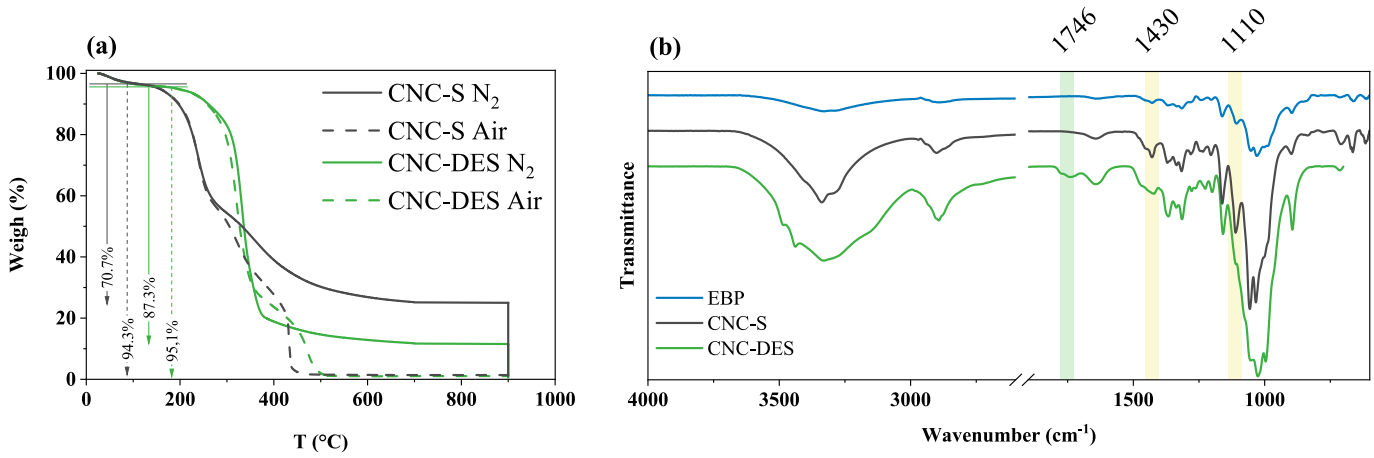

Fig. 3. CNC characterization, (a) TGA, (b) FT-IR.

CNC-S presents two absorption bands at 1430 cm^{-1} and 1110 cm^{-1} related to S═O stretching. C—S lays in the range 700–600 cm^{-1}, however, the absorption is weak and the position may vary; thus, this band has little value in the determination of the structure (Silverstein & Webster, 1998). CNC-DES also presents the —COOR and —COOH superimposed band, at around 1740 cm^{-1}. According to Sirviö et al. (2016), it is common to observe this overlapping.

3.2. Sustainability evaluation through ESCAPE tool

We identified six case studies, each involving a specific combination of electricity sources (Fig. 4) and water types used in the purification steps. These case studies were designed to evaluate the environmental impact of different production setups, using Italy, France, and a European average as benchmarks for electrical consumption, reflecting the geographic locations of the experiments. For a proper evaluation of the energy mix impact, its variation along the years was considered for the three geographical scenarios from 2008 up today (Fig. 4). In all cases, the contribution of renewable sources has significantly increased in the last 17 years. In the case of Italy this happened by replacing fossil fuel source, while for France the contribution of fossil fuel remained constant, with a limited reduction of nuclear sources in favor of the renewable ones. The change in energy mixes resulted in different EE and CF ESCAPE indicators. Fig. S2 reports the correlation between energy mix and EE/CF indicators following the trend for three different years (2008, 2018 and 2025). A decrease of the indicators' values is evident, especially for the Italian scenario, due to the higher increase of renewable sources. On the other hand, the overall stability in French energy mix showed almost constant indicators.

The type of water used in the laboratory activities varied: deionized water in Italy, distilled water in France, and tap water included to simulate potential industrial-scale production environments in the eco-redesign step.

The case studies (CS) were defined as follows:

- **CS 1**: Production and electricity consumption both in Italy, deionized water.
- **CS 2**: Production in Italy with European average electricity consumption, deionized water.
- **CS 3**: Production and electricity consumption both in France, distilled water.
- **CS 4**: Production in France with European average electricity consumption, distilled water.
- **CS 5 and 6**: These scenarios explore the use of tap water for production processes, with electricity sourced respectively from Italy and France.

Due to the long purification time, it was decided to investigate the differences between the EE and CF in a scenario where the dialysis water was maintained under stirring and a scenario where no stirring was adopted. The mass recovery after lyophilization was considered 22 % for the H_2SO_4 process, and 65 % for DES based method. However, as previously stated, to better evaluate the impact of other production aspects and to consider processes starting from different sources and possibly higher yields, we also considered scenarios where the mass recovery was assumed to be 100 %. Each scenario is defined as follows:

A) 100 % mass recovery, dialysis stirred
B) 100 % mass recovery, dialysis not stirred
C) X% mass recovery, dialysis stirred
D) X% mass recovery, dialysis not stirred

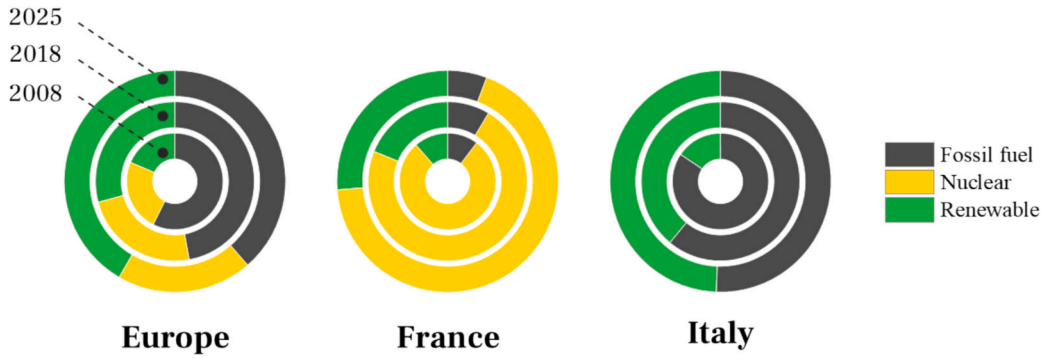

Fig. 4. Italian, French, and European energy mix throughout the years (Graham et al., 2025; International Energy Agency, 2008, 2018a, 2018b).

Fig. 5 reports the comparison in terms of EE (a and b) and CF (c and d) between CNC-S (a and c) and CNC-DES (b and d) productions for CS 1–4, by considering all four A-D scenarios just described. The results unequivocally demonstrate the superior sustainability of DES-based extractions over H_2SO_4-based ones for each scenario and case study. As expected, the difference is lower when mass recovery is not considered, and no mixing occurs during dialysis (scenario B). In this case the parameters span from 331 MJ and 16.51 $kgCO_{2eq}$ for H_2SO_4-based hydrolysis to 246 MJ and 12.5 $kgCO_{2eq}$ for DES-based treatment. Interestingly, these values are significantly lower than those determined with 2018 data (357 MJ and 19.7 $kgCO_{2eq}$ for H_2SO_4-mediated hydrolysis against 263.8 MJ and 17.8 $kgCO_{2eq}$ of the DES-based treatment). For a more detailed comparison, Fig. S3 reports the comparison of the four A–D scenarios for case studies 1–4 referred to 2018. The disparity significantly peaks when both 22 % (H_2SO_4) and 65 % (DES) mass recoveries are factored in (scenarios C and D). Even though we should once again underline that the products present different chemical and physical properties, CNC-DES production emerges as more sustainable than H_2SO_4-based one. The availability of environmental impact data for DES is significant, given its extensive study in cellulose extraction techniques, although research on DES extraction of waste products for CNC production remains limited (Chia et al., 2024).

Furthermore, it has already been reported how geographical variations significantly influence greenhouse gas (GHG) emissions during CNC production (Hao et al., 2023).

In terms of geography, this study identifies France as the most sustainable location for CNC production (case study 3, Fig. 5), owing to its energy mix, which is 34 % less carbon-intensive than the European average mix. Moreover, mixing during dialysis after centrifugation can notably impact the process, increasing EE and CF by an average of 41 % (Scenarios A and C, Fig. 5). These findings underline how sustainability is strongly influenced by the energy mix of the country where the process is performed. While France remains one of the most sustainable options due to its low-carbon electricity, recent data suggest that other countries are progressively increasing the share of renewable energy in their national mixes. In particular, Italy has increased its use of renewable energy by 17 % compared to pre-COVID-19 levels, with wind and solar power contributing 28 % more than before. This positive trend is likely influenced by the implementation of the National Recovery and Resilience Plan (PNRR), which has supported the country's transition toward cleaner energy sources.

Fig. S4 shows how the EE is distributed between raw materials and production. It is possible to notice how much the freeze-drying step impacts the production, followed by the purification step, both in terms of electricity employed for dialysis stirring and of water usage and consumption. Comparing the weight that the purification step has for both the production routes, the lower process times and the lower volumes of water consumed make the DES-based product have a lower percentile impact on total EE.

Radar plots in Fig. 6 depict the four parameters considered in the ESCAPE tool, with a logarithmic scale emphasizing the impact of electricity used to run devices on the total process (see Fig. S5 for a comparison with 2018 data). Lyophilization emerges as the most impactful process, followed by water consumption and electricity for heating plates, with raw materials exerting the least influence. In DES-based production, electricity usage tops the consumption parameter, followed by raw materials, electricity for heating, and water usage. Notably, water usage in both processes does not exceed 35 L for treating 1 g of pretreated bleached cellulose.

Literature indicates that 130 kg of deionized water without acid recovery is consumed for bleached wood pulp, while electricity consumption is reported at 3.38 kWh, and H_2SO_4 consumption at 6.35 kg per kg of CNC (Rajendran et al., 2023), compared to this study's findings of 4.54 kWh, of which 4.4 kWh are attributed to the purification process.

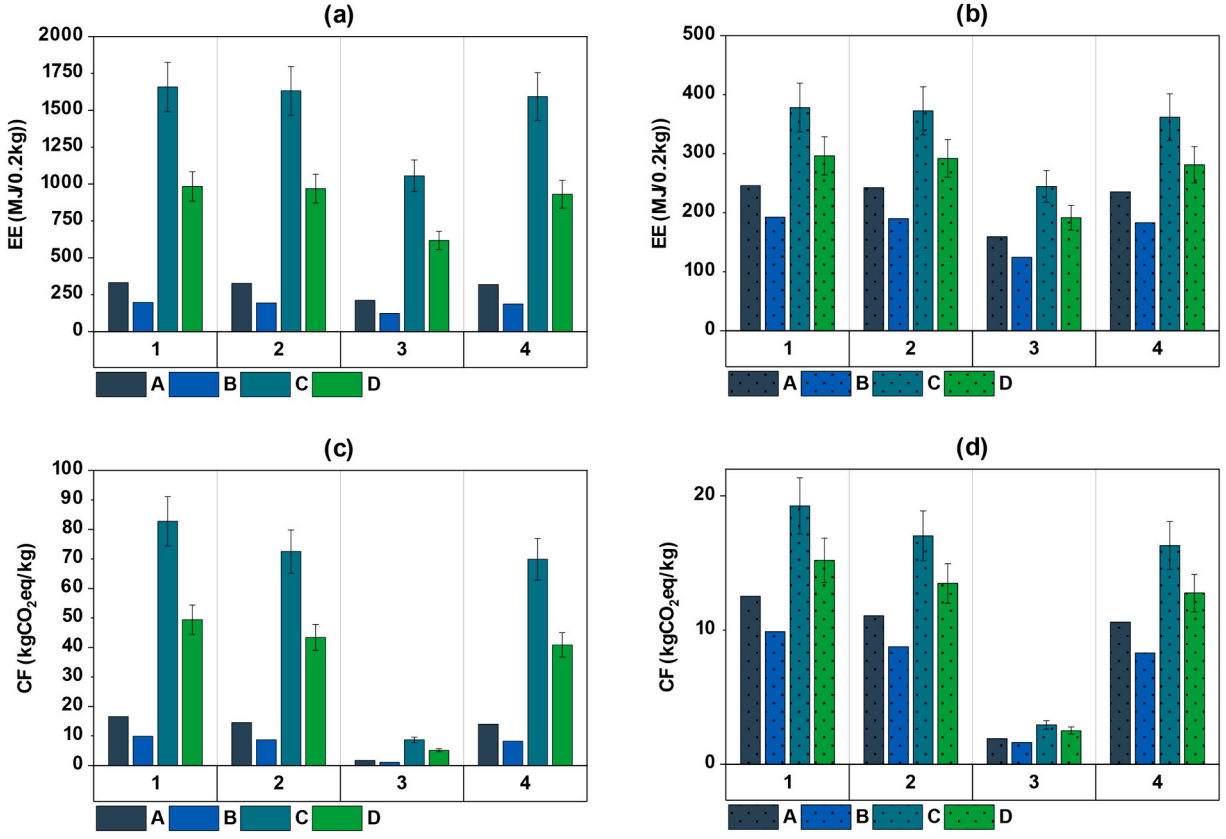

Fig. 5. Comparison of four A–D scenarios for CS 1–4. (a) Total EE for H_2SO_4 treatment; (b) total EE for DES treatment; (c) total CF for H_2SO_4 treatment; (d) total CF for DES-based treatment.

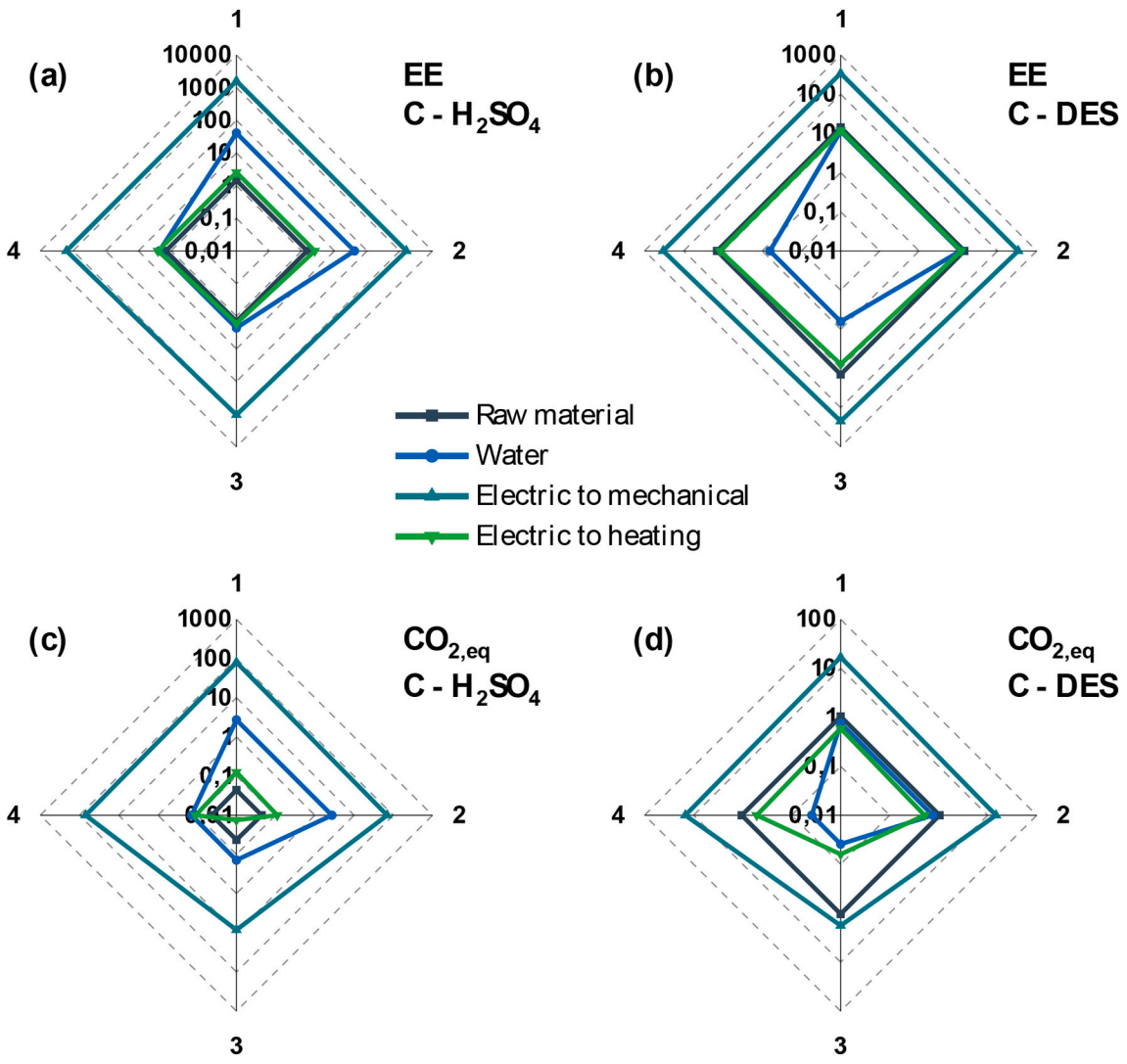

Fig. 6. Radar plot of scenario C. (a) EE of H_2SO_4 method, (b) EE of DES method, (c) CF of H_2SO_4 method, (d) CF of DES method.

Optimization of the purification process focuses on the centrifugation stage, as reported by Zhang et al. (2022), which demonstrates significant improvements achievable through microfiltration, resulting in a 40 % reduction in global warming potential and a 48 % decrease in non-renewable energy consumption. These improvements are mainly attributed to higher recovery ratios (65 %), acid concentration, and reduced water consumption.

The study by Zhang et al. (2022) also highlights the global warming impact of CNC produced from cotton pulp, ranging from 29.6 to 49.4 kg CO_2 eq/kg of CNC depending on the filtration process.

In another industrial case study (Hao et al., 2023), GHG emissions values for CNC with 61 % and 64 % concentrations of H_2SO_4 products are reported at 12.6 $kgCO_{2eq}$/kgCNC and 16.6 $kgCO_{2eq}$/kgCNC, respectively.

Leão et al. (2017) conducted LCAs for gate-to-gate processes of CNC production, focusing on a functional unit of 1 kg of nanocellulose, and identified twelve scenarios for nanocrystal extraction, including treatment with sodium hydroxide or sodium chlorite followed by H_2SO_4 hydrolysis. Their study on nanocellulose production from sugarcane bagasse, including bleaching pretreatment and 30 min of H_2SO_4 (64 %) hydrolysis, resulted in sequences yielding 67 % and 53 % crystallinity, with associated carbon footprints of 23.5 $kgCO_{2eq}$/kg nanocellulose and 13.7 $kgCO_{2eq}$/kg nanocellulose, respectively. In our best-case scenario (case study 3), H_2SO_4-based processes account for 8 kg CO_{2eq}/kg of nanocellulose, achieving a higher crystallinity of 86 % compared to 67 %. The data were collected without performing calculations as foreground data for the upstream pretreatment relative to the bleaching stage, instead, we utilized Simapro software background data for the EBP.

As ESCAPE outputs highlight the significant impact of water usage and consumption on the overall CNC production, we decided to explore the hypothetical use of tap water in place of the deionized and distilled one, in order to evaluate the possible positive impact on overall EE and CF parameters.

The bar chart reported in Fig. 7 depicts the comparison between EE and CF for the Italian (CS 1 and 5) and French (CS 3 and 6) production, juxtaposing the effect of stirring (scenario C) and not-stirring (scenario D), when considering mass recovery, before (CS 1 and 3) and after (CS 5 and 6) optimization by using tap water (see Fig. S6 for a comparison with 2018 data).

The EE for H_2SO_4 based production (Fig. 7a, blue) decreased by an average of 40 %, while DES based one (green) showed a 20 % decrease (see Fig. S5 for a comparison with 2018). This difference is due to the different impact that stirring had on both processes. In fact, as the radar and bar plots (Fig. 6 and Fig. 7) showed, both electricity and water had an important impact on final EE. Furthermore, the different decrease is also supported by the different weights that the purification step had on the final EE. This important decrease is not observed in CF (Fig. 7b), due

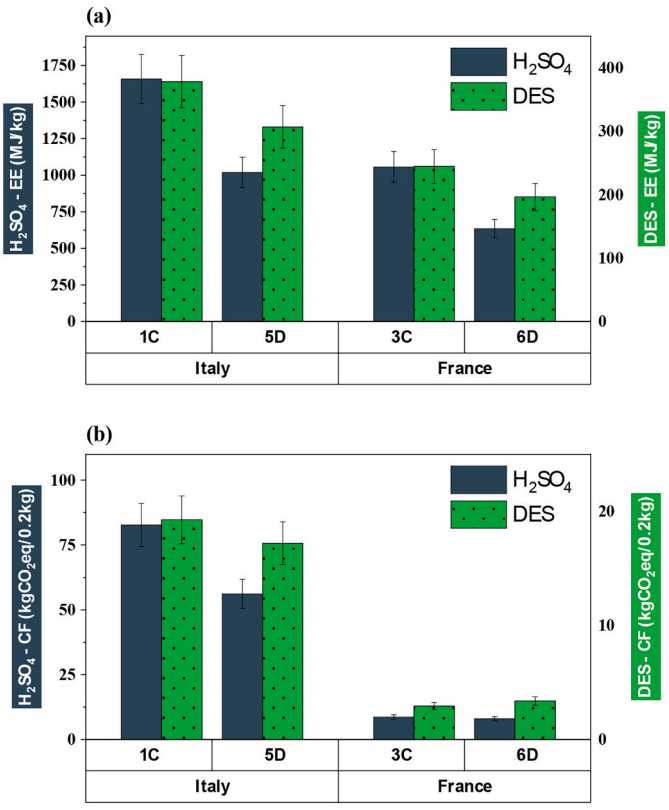

Fig. 7. (a) EE change after reaction optimization; (b) CF after reaction optimization.

to the lower impact that water has on final CF. In particular, Fig. S7 shows the contribution in EE decrease by switching from distilled or deionized water to tap water. It is clear that the change in water has a high impact on CNC-H_2SO_4 production, due to the higher water usage for this synthesis, but it represents an important EE decrease for the DES-based production as well.

The progressive decarbonization of national electricity grids, as observed in several European countries, could further reduce the environmental impact of the synthesis processes. These changes should be considered when interpreting ESCAPE results over time, as local infrastructure improvements can significantly affect embodied energy and carbon footprint assessments. In this context, national and European strategies promoting energy efficiency and renewable energy deployment may indirectly support more sustainable material development also at early research stages.

3.3. Products' morphological characterization to validate the eco-design approach

On the basis of the outputs derived from ESCAPE optimization analysis, which highlighted the advantages in terms of sustainability by operating with, we decided to implement the use of tap water and avoiding stirring during dialysis in the synthetic procedures for both CNC-S and CNC-DES, in order confirm that the corresponding CNS-S-TAP and CNC-DES-TAP samples maintained the same morphological characteristics.

The stability of colloidal dispersions was evaluated by measuring ζ-potential (Table 2). CNC-S showed lower ζ-potential values, due to the negative charges introduced by the H_2SO_4 treatment, resulting in a more stable suspension. Meanwhile, CNC-DES presented higher ζ-potential, even if still negative, due to the presence of —COOH moieties deriving from the grafting of the cellulosic surface by OxAc, which may have some impact on the superficial charge. As expected, after the introduction of tap water in CNC production, the overall charge changed. For CNC-S-TAP, ζ-potential increased by 45 %, while for CNC-DES-TAP, ζ-potential increased by almost 24 %. This different increment is probably owed to the surface charge of CNC-S, which tends to attract more positive ions than the lower charged CNC-DES.

Table 2
ζ-potential of EBP, CNC-S, CNC-DES, CNC-S-TAP and CNC-DES-TAP.

Entry	ζ-potential (mV)
EBP	−10.69 ± 5.487
CNC-S	−53.2 ± 3.680
CNC-DES	−36.03 ± 1.640
CNC-S-TAP	−29.04 ± 1.007
CNC-DES-TAP	−27.48 ± 1.098

SEM-EDX analysis conducted on CNS-S-TAP and CNS-DES-TAP samples confirmed the presence of common mono-, di- and trivalent ions, including Cl^-, Na^+, K^+, Ca^{2+}, Mg^{2+}, Si^{2+}, Al^{3+}, all of them almost absent in EBP sample (Figs. S8–S10).

AFM confirmed the production of CNC. Fig. 8 (a–b) show the never-dried crystals after the purification step. The main difference between the two sets of samples consists in the aggregation of CNC which, together with the shape of the crystal, reveals the degree of hydrolysis. CNC-S present lower aggregation, and higher degree of hydrolysis, which is due to the higher acidity of the reaction environment, and the higher charge on the nanocrystal surface, as revealed by ζ-potential analyses. The average length is 166 ± 71.9 nm, in line with Eucalyptus CNC reported in the literature (Beck-Candanedo et al., 2005; De Mesquita et al., 2010). On the other hand, CNC-DES poses a challenge for statistical data due to their aggregation. However, it is still possible to see the nanoscale, with a length in the range of 90–250 nm and the width in the range of 9–30 nm.

TEM images (Fig. 8 c–d) were also collected to better define crystals' dimension and morphology. For CNC-S the average length is 122 ± 42.0 nm. Once again, CNC-DES surface is not charged, and this makes them difficult to disperse. However, it is possible to assess qualitatively the presence of CNC. Even though it is difficult to perform a statistical analysis, it is possible to notice that length and width are in the range of 100–220 nm and 5–10 nm, respectively. CNC dimensions may slightly differ from TEM results due to the AFM tip broadening effect, which misrepresents the CNC borders.

After optimization, to prove the unchanged morphology of CNC obtained, further TEM analyses were conducted. CNC-S-TAP showed an average length of 120 ± 37.9 nm (Fig. 8e). Once again, this result should be ascribed to the presence of tap water ions, which increase superficial charge and limit the repulsion between single crystals. Even though H_2SO_4 based production leads to lower mass recoveries, it should be noticed that the extraction process results in better defined and dispersed CNC, whereas DES based extraction produces more aggregated CNC and leaves some fibrous portions.

The crystallinity index (CI%) was evaluated using the Segal method (Segal et al., 1959). The XRD patterns of EBP and CNC are depicted in Fig. S11 and they show the typical cellulose Iβ diffractogram. Cellulose Iβ crystalline peaks are at $2\Theta = 14.9°$, $16.5°$, $22.5°$, whereas the amorphous valley is $2\Theta = 20.7°$. The starting material presented a crystallinity index of 88.37 %, CNC-S of 88.6 %, and CNC-DES of 83.3 %, which are considered highly crystalline (Vanderfleet & Cranston, 2021). Once the process was optimized using tap water, further XRD analyses were performed. The diffractograms reported in Fig. S11 show the new cellulose Iβ patterns. CNC-S-TAP presented a decrease in CI% to 79.2 %, whereas CNC-DES-TAP had a decrease in CI% to 79.5 %. Overall, the crystallinity index did not change drastically.

In summary, our study identified that freeze-drying and purification are the most impactful steps in the reaction process. Specifically, water usage for dialysis and the extended stirring duration exhibited the

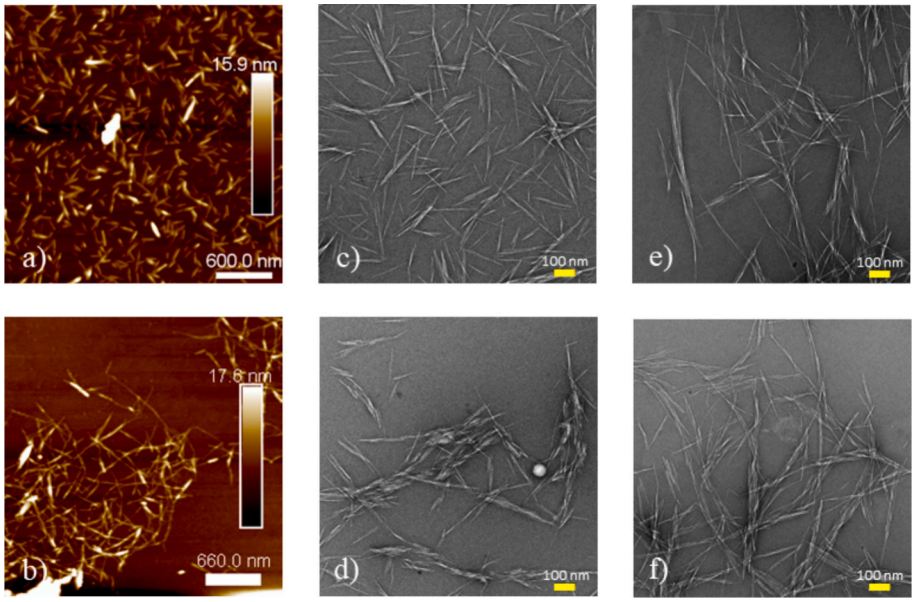

Fig. 8. (a) AFM of CNC-S; (b) AFM of CNC-DES; (c) TEM of CNC-S; (d) TEM of CNC-DES; (e) TEM of CNC S-TAP; (f) TEM of CNC-DES-TAP.

highest EE and CF. Analyzing the impact by country energy mix, Italy would need to achieve 91 % renewables in its energy mix, predominantly nuclear energy, to match the more sustainable practices of France. Notably, similar findings have been observed in industrial level sustainability assessments, such as the production of vanillin. Recent studies (Zhao et al., 2021) highlighted that vanillin synthesis involves high water consumption via industrial oxidation and biotechnological processes. Effective methods to reduce chemical consumption included recovering organic solvents and substituting ultrapure water with industrial or distilled water.

4. Conclusions

In this work, we present the eco-design of CNC production, introducing the innovative application of the ESCAPE method to two experimental processes. The processes involve the most common H_2SO_4-based extraction, and the claimed "more sustainable" DES-based one. From these analyses, we have revealed that the most impactful steps during the reaction process are freeze-drying, which unfortunately can't be optimized, and purification. In particular, the use of water for dialysis and stirring during the days had the highest EE and CF. Consequently, the eco-design analysis revealed that stirring during dialysis should be avoided, and distilled water should be substituted with tap water. From an upscaling perspective, using tap water is advantageous. The EE for CNC-S/CNC-S-TAP production decreased by about 40 %, whereas for CNC-DES/CNC-DES-TAP the decrease was around 20 %.

Furthermore, the chemical, physical, and morphological properties of CNC were investigated before and after ESCAPE-driven optimization. The CNC surface chemistry was investigated by means of FT-IR, and both the presence of sulfate groups on CNC-S surface and the presence of oxalate on CNC-DES surface were proved. We checked the thermal stability of CNC produced with distilled or deionized water, showing the common CNC behavior. Their rod-like shape and dimension were investigated by TEM and AFM analyses (in the length range of 100–300 nm). The colloidal stability of the suspensions was assessed, and it decreased when tap water was introduced, while the CI% was not significantly impacted. It is possible to conclude that by exploiting tap water and avoiding stirring, the production routes were improved consistently without affecting the characteristics of final products. Employing simplified tools to assess the sustainability of synthesis processes at the lab scale can offer advantages by minimizing or avoiding complex technology optimizations required at a larger scale.

CRediT authorship contribution statement

Gloria Nicastro: Writing – original draft, Visualization, Validation, Methodology, Investigation, Data curation, Conceptualization. **Ario Fahimi:** Writing – original draft, Visualization, Validation, Methodology, Investigation, Data curation. **Alain Dufresne:** Writing – review & editing, Supervision, Resources. **Ehsan Vahidi:** Resources. **Carlo Punta:** Writing – review & editing, Validation, Supervision, Methodology, Conceptualization. **Elza Bontempi:** Writing – review & editing, Validation, Supervision, Methodology.

Fundings

This work was supported by the Next-GenerationEU (Italian PNRR – M4 C2, Invest 1.3 – D.D. 1551.11-10-2022, PE00000004) within the MICS (Made in Italy – Circular and Sustainable) Extended Partnership.

Declaration of competing interest

The authors declare that they have no known competing financial interests or personal relationships that could have appeared to influence the work reported in this paper.

Acknowledgments

We thank the NanoBio-ICMG Platform (UAR 2607, Grenoble) for granting access to the electron microscopy facility. LGP2 is part of the LabEx Tec 21 (Investissements d'Avenir - grant agreement n°ANR-11-LABX-0030) and of the PolyNat Carnot Institut (Investissements d'Avenir - grant agreement n°ANR-11-CARN-030-01). C.P. and G.N thank the contribution of the Italian Ministry of University and Research (MUR) under the PON Research and Innovation 2014–2020 program (Action IV.5 – Doctorates on green topics).

Appendix A. Supplementary data

Supplementary data to this article can be found online at https://doi.org/10.1016/j.carbpol.2025.124310.

Data availability

Data will be made available on request.

References

Abbott, A. P., Boothby, D., Capper, G., Davies, D. L., & Rasheed, R. K. (2004). Deep eutectic solvents formed between choline chloride and carboxylic acids: Versatile alternatives to ionic liquids. *Journal of the American Chemical Society, 126*(29), 9142–9147. https://doi.org/10.1021/ja048266j

Aguayo, M. G., Pérez, A. F., Reyes, G., Oviedo, C., Gacitúa, W., Gonzalez, R., & Uyarte, O. (2018). Isolation and characterization of cellulose nanocrystals from rejected fibers originated in the Kraft Pulping process. *Polymers, 10*(10). https://doi.org/10.3390/polym10101145

Amoroso, R., Hollmann, F., & Maccallini, C. (2021). Choline chloride-based des as solvents/catalysts/chemical donors in pharmaceutical synthesis. *Molecules, 26*(20). https://doi.org/10.3390/molecules26206286

Azeredo, H. M. C., Rosa, M. F., & Mattoso, L. H. C. (2017). Nanocellulose in bio-based food packaging applications. *Industrial Crops and Products, 97*, 664–671. https://doi.org/10.1016/j.indcrop.2016.03.013

Beck-Candanedo, S., Roman, M., & Gray, D. G. (2005). Effect of reaction conditions on the properties and behavior of wood cellulose nanocrystal suspensions. *Biomacromolecules, 6*(2), 1048–1054. https://doi.org/10.1021/bm049300p

Besbes, I., Alila, S., & Boufi, S. (2011). Nanofibrillated cellulose from TEMPO-oxidized eucalyptus fibres: Effect of the carboxyl content. *Carbohydrate Polymers, 84*(3), 975–983. https://doi.org/10.1016/j.carbpol.2010.12.052

Bontempi, E. (2017). A new approach for evaluating the sustainability of raw materials substitution based on embodied energy and the CO2 footprint. *Journal of Cleaner Production, 162*, 162–169. https://doi.org/10.1016/J.JCLEPRO.2017.06.028

Bontempi, E. (2022). How to perform a material recovery sustainability evaluation preliminary to LCA? *Resources, Environment and Sustainability, 9*(July), Article 100074. https://doi.org/10.1016/j.resenv.2022.100074

British Standards. (2020). *BSI Standards Publication Environmental management — Life cycle assessment — Principles and framework. Bs En Iso 14040, August 2006*.

Carrillo, I., Mendonça, R. T., Ago, M., & Rojas, O. J. (2018). Comparative study of cellulosic components isolated from different Eucalyptus species. *Cellulose, 25*(2), 1011–1029. https://doi.org/10.1007/s10570-018-1653-2

Ceylan, Ö., Van Landuyt, L., Rahier, H., & De Clerck, K. (2013). The effect of water immersion on the thermal degradation of cotton fibers. *Cellulose, 20*(4), 1603–1612. https://doi.org/10.1007/s10570-013-9936-0

Chen, K., Liang, Y., Hu, Z., & Shen, J. (2024). Cellulose nanocrystals supported ternary alloy nanoclusters catalysts for efficient hydrogen production from formic acid. *Molecular Catalysis, 553*(October 2023), Article 113742. https://doi.org/10.1016/j.mcat.2023.113742

Chen, L., Wang, Q., Hirth, K., Baez, C., Agarwal, U. P., & Zhu, J. Y. (2015). Tailoring the yield and characteristics of wood cellulose nanocrystals (CNC) using concentrated acid hydrolysis. *Cellulose, 22*(3), 1753–1762. https://doi.org/10.1007/s10570-015-0615-1

Chia, M. R., Phang, S. W., Mohd Razali, N. S., & Ahmad, I. (2024). Approach towards sustainable circular economy: Waste biorefinery for the production of cellulose nanocrystals. *Cellulose, 31*(6). https://doi.org/10.1007/s10570-024-05825-9. Springer Netherlands.

Ciolacu, D., Ciolacu, F., & Popa, V. I. (2011). Amorphous cellulose structure and characterization. Cellulose chemistry and technology. *Cellulose Chemistry Technology, 45*(2), 13–21.

Corsi, I., Venditti, I., Trotta, F., & Punta, C. (2023). Environmental safety of nanotechnologies: The eco-design of manufactured nanomaterials for environmental remediation. *Science of the Total Environment, 864*(December 2022), Article 161181. https://doi.org/10.1016/j.scitotenv.2022.161181

da Cruz, Las-Casas, B., Riberio Dias, & Arantes, V. (2024). Nanocelluloses as sustainable emerging technologies: State of the art and future challenges based on life cycle assessment. *Sustainable Materials and Technologies, 41*, Article e01010. https://doi.org/10.1016/j.susmat.2024.e01010

De Mesquita, J. P., Donnici, C. L., & Pereira, F. V. (2010). Biobased nanocomposites from layer-by-layer assembly of cellulose nanowhiskers with chitosan. *Biomacromolecules, 11*(2), 473–480. https://doi.org/10.1021/bm9011985

Di Giorgio, L., Martín, L., Salgado, P. R., & Mauri, A. N. (2020). Synthesis and conservation of cellulose nanocrystals. *Carbohydrate Polymers, 238*(December 2019), Article 116187. https://doi.org/10.1016/j.carbpol.2020.116187

Dong, H., Strawhecker, K. E., Snyder, J. F., Orlicki, J. A., Reiner, R. S., & Rudie, A. W. (2012). Cellulose nanocrystals as a reinforcing material for electrospun poly(methyl methacrylate) fibers: Formation, properties and nanomechanical characterization. *Carbohydrate Polymers, 87*(4), 2488–2495. https://doi.org/10.1016/j.carbpol.2011.11.015

Douard, L., Belgacem, M. N., & Bras, J. (2022). Extraction of carboxylated nanocellulose by combining mechanochemistry and NADES. *ACS Sustainable Chemistry and Engineering, 10*(39), 13017–13025. https://doi.org/10.1021/acssuschemeng.2c02783

Ducoli, S., Zacco, A., Valentim, B., Zanoletti, A., Ye, G., Mousa, E., & Bontempi, E. (2023). ESCAPE simplified approach designed to evaluate materials sustainability: The case of new adsorbent materials for activated carbon substitution. *Sustainable Materials and Technologies, 38*(September), Article e00709. https://doi.org/10.1016/j.susmat.2023.e00709

Esposito, M. C., Riva, L., Russo, G. L., Punta, C., Corsi, I., Tosti, E., & Gallo, A. (2024). Reproductive toxicity assessment of cellulose nanofibers, citric acid, and branched polyethylenimine in sea urchins: Eco-design of nanostructured cellulose sponge framework (part B). *Environmental Pollution, 350*, Article 123934. https://doi.org/10.1016/j.envpol.2024.123934

Fahimi, A., Ducoli, S., Federici, S., Ye, G., Mousa, E., Frontera, P., & Bontempi, E. (2022). Evaluation of the sustainability of technologies to recycle spent lithium-ion batteries, based on embodied energy and carbon footprint. *Journal of Cleaner Production, 338*(December 2021), 130493. https://doi.org/10.1016/j.jclepro.2022.130493

Gil-Castell, O., Reyes-Contreras, P., Barra, P. A., Mendonça, R. T., Carrillo-Varela, I., Badia, J. D., … Ribes-Greus, A. (2022). The role of Eucalyptus species on the structural and thermal performance of cellulose nanocrystals (CNCs) isolated by acid hydrolysis. *Polymers, 14*(3). https://doi.org/10.3390/polym14030423

Graham, E., Fulghum, N., & Altieri, K. (2025). Global electricity review 2025. https://ember-energy.org/latest-insights/global-electricity-review-2025/#executive-summary.

Habibi, Y., Lucia, L. A., & Rojas, O. J. (2010). Cellulose nanocrystals: Chemistry, self-assembly, and applications. *Chemical Reviews, 110*(6), 3479–3500. https://doi.org/10.1021/cr900339w

Hao, Z., Hamad, W. Y., & Yaseneva, P. (2023). Understanding the environmental impacts of large-scale cellulose nanocrystals production: Case studies in regions dependent on renewable and fossil fuel energy sources. *Chemical Engineering Journal, 478*(November), Article 147160. https://doi.org/10.1016/j.cej.2023.147160

Hoo, D. Y., Tang, S. Y., Kikuchi, Y., Ng, B. J., Foo, C. Y., Tan, K. W., & Tan, J. (2024). Prospective life cycle assessment: Identifying the most promising methods for sustainable cellulose nanocrystal production. *Chemical Engineering Journal, 498*. https://doi.org/10.1016/j.cej.2024.154964

International Energy Agency. (2008). *Electricity information 2008*. Organization for Economic Cooperation & Development Turpin Distribution Services Limited [distributor].

International Energy Agency. (2018a). *Electricity information* (pp. 1–708). IEA Statistics. https://doi.org/10.1787/electricity-2018-en

International Energy Agency. (2018b). *World summary energy balances (2018 edition)*. https://doi.org/10.1787/world_energy_bal-2018-en

ISO. (2010). ISO 5351-2010 pulps-determination of limiting viscosity number in cupri-ethylenediamine (CED) solution. *1199*(50), 23.

Leão, R. M., Miléo, P. C., Maia, J. M. L. L., & Luz, S. M. (2017). Environmental and technical feasibility of cellulose nanocrystal manufacturing from sugarcane bagasse. *Carbohydrate Polymers, 175*, 518–529. https://doi.org/10.1016/j.carbpol.2017.07.087

Li, F., Biagioni, P., Bollani, M., Maccagnan, A., & Piergiovanni, L. (2013). Multi-functional coating of cellulose nanocrystals for flexible packaging applications. *Cellulose, 20*(5), 2491–2504. https://doi.org/10.1007/s10570-013-0015-3

Liu, A., Wu, H., Naeem, A., Du, Q., Ni, B., Liu, H., Li, Z., & Ming, L. (2023). Cellulose nanocrystalline from biomass wastes: An overview of extraction, functionalization and applications in drug delivery. *International Journal of Biological Macromolecules, 241*(April), Article 124557. https://doi.org/10.1016/j.ijbiomac.2023.124557

Liu, Q., Yuan, T., Fu, Q.j., Bai, Y.y., Peng, F., & Yao, C.l. (2019). Choline chloride-lactic acid deep eutectic solvent for delignification and nanocellulose production of moso bamboo. *Cellulose, 26*(18), 9447–9462. https://doi.org/10.1007/s10570-019-02726-0

Mendoza, D. J., Maliha, M., Raghuwanshi, V. S., Browne, C., Mouterde, L. M. M., Simon, G. P., … Garnier, G. (2021). Diethyl sinapate-grafted cellulose nanocrystals as nature-inspired UV filters in cosmetic formulations. *Materials Today Bio, 12*(August), Article 100126. https://doi.org/10.1016/j.mtbio.2021.100126

Ong, K. J., Shatkin, J. A., Nelson, K., Ede, J. D., & Retsina, T. (2017). Establishing the safety of novel bio-based cellulose nanomaterials for commercialization. *NanoImpact, 6*, 19–29. https://doi.org/10.1016/j.impact.2017.03.002

Pennells, J., Godwin, I. D., Amiralian, N., & Martin, D. J. (2020). Trends in the production of cellulose nanofibers from non-wood sources. *Cellulose, 27*, 575–593. https://doi.org/10.1007/s10570-019-02828-9

Rajendran, N., Runge, T., Bergman, R. D., Nepal, P., & Houtman, C. (2023). Techno-economic analysis and life cycle assessment of cellulose nanocrystals production from wood pulp. *Bioresource Technology, 377*(March), Article 128955. https://doi.org/10.1016/j.biortech.2023.128955

Rana, A. K., Frollini, E., & Thakur, V. K. (2021). Cellulose nanocrystals: Pretreatments, preparation strategies, and surface functionalization. *International Journal of Biological Macromolecules, 182*, 1554–1581. https://doi.org/10.1016/j.ijbiomac.2021.05.119

Riva, L., Dotti, A., Iucci, G., Venditti, I., Meneghini, C., Corsi, I., … Battocchio, C. (2024). Silver nanoparticles supported onto TEMPO-oxidized cellulose nanofibers for promoting Cd2+ cation adsorption. *ACS Applied Nano Materials, 7*(2), 2401–2413. https://doi.org/10.1021/acsanm.3c06052

Roman, M., & Winter, W. T. (2004). Effect of sulfate groups from sulfuric acid hydrolysis on the thermal degradation behavior of bacterial cellulose. *Biomacromolecules, 5*(5), 1671–1677. https://doi.org/10.1021/bm034519+

Roohani, M., Habibi, Y., Belgacem, N. M., Ebrahim, G., Karimi, A. N., & Dufresne, A. (2008). Cellulose whiskers reinforced polyvinyl alcohol copolymers nanocomposites. *European Polymer Journal, 44*(8), 2489–2498. https://doi.org/10.1016/j.eurpolymj.2008.05.024

Rusconi, T., Riva, L., Punta, C., Solé, M., & Corsi, I. (2024). Environmental safety of nanocellulose: An acute in vivo study with marine mussels Mytilus galloprovincialis. *Environmental Science: Nano, 11*(1), 61–77. https://doi.org/10.1039/d3en00135k

Segal, L., Creely, J. J., Martin, A. E., & Conrad, C. M. (1959). An empirical method for estimating the degree of crystallinity of native cellulose using the X-ray

diffractometer. *Textile Research Journal, 29*(10), 786–794. https://doi.org/10.1177/004051755902901003

Silverstein, R. M., & Webster, F. X. (1998). *Spectrometric identification of organics compounds* (6th ed.). John Wiley and Sons Inc.

Sirviö, J. A., Visanko, M., & Liimatainen, H. (2016). Acidic deep eutectic solvents as hydrolytic media for cellulose nanocrystal production. *Biomacromolecules, 17*(9), 3025–3032. https://doi.org/10.1021/acs.biomac.6b00910

Tang, Y., Yang, H., & Vignolini, S. (2022). Recent progress in production methods for cellulose nanocrystals: Leading to more sustainable processes. *Advanced Sustainable Systems, 6*(3). https://doi.org/10.1002/adsu.202100100

Trache, D., Hussin, M. H., Haafiz, M. K. M., & Thakur, V. K. (2017). Recent progress in cellulose nanocrystals: Sources and production. *Nanoscale, 9*(5), 1763–1786. https://doi.org/10.1039/c6nr09494e

Vanderfleet, O. M., & Cranston, E. D. (2021). Production routes to tailor the performance of cellulose nanocrystals. *Nature Reviews Materials, 6*(2), 124–144. https://doi.org/10.1038/s41578-020-00239-y

Wang, H., Li, J., Zeng, X., Tang, X., Sun, Y., Lei, T., & Lin, L. (2020). Extraction of cellulose nanocrystals using a recyclable deep eutectic solvent. *Cellulose, 27*(3), 1301–1314. https://doi.org/10.1007/s10570-019-02867-2

Wang, Z., Song, L., Ye, N., Yu, Q., Zhai, Y., Zhang, F., … Peijnenburg, W. J. G. M. (2020). Oxidative stress actuated by cellulose nanocrystals and nanofibrils in aquatic organisms of different trophic levels. *NanoImpact, 17*, Article 100211. https://doi.org/10.1016/j.impact.2020.100211

Xu, Q., Poggi, G., Resta, C., Baglioni, M., & Baglioni, P. (2020). Grafted nanocellulose and alkaline nanoparticles for the strengthening and deacidification of cellulosic artworks. *Journal of Colloid and Interface Science, 576*, 147–157. https://doi.org/10.1016/j.jcis.2020.05.018

Zargar, S., Jiang, J., Jiang, F., & Tu, Q. (2022). Isolation of lignin-containing cellulose nanocrystals: Life-cycle environmental impacts and opportunities for improvement. *Biofuels, Bioproducts and Biorefining, 16*(1), 68–80. https://doi.org/10.1002/bbb.2261

Zhang, L., Jia, X., Ai, Y., Huang, R., Qi, W., He, Z., … Su, R. (2022). Greener production of cellulose nanocrystals: An optimised design and life cycle assessment. *Journal of Cleaner Production, 345*. https://doi.org/10.1016/j.jclepro.2022.131073

Zhao, X., Zhang, Y., Cheng, Y., Sun, H., Bai, S., & Li, C. (2021). Identifying environmental hotspots and improvement strategies of vanillin production with life cycle assessment. *Science of the Total Environment, 769*, Article 144771. https://doi.org/10.1016/j.scitotenv.2020.144771